PHYSICAL REVIEW B **74**, 161303(R) (2006)

Revivals, collapses, and magnetic-pulse generation in quantum rings

A. S. Moskalenko,* A. Matos-Abiague, and J. Berakdar
Max-Planck Institut für Mikrostrukturphysik, Weinberg 2, 06120 Halle, Germany
(Received 12 September 2006; published 18 October 2006)

Using a microscopic theory based on the density-matrix formalism we investigate quantum revivals and collapses of the charge polarization and charge current dynamics in mesoscopic rings driven by short asymmetric electromagnetic pulses. The collapsed state is utilized for subpicosecond switching of the current and associated magnetization, enabling thus the generation of pulsed magnetic fields with a tunable time structure and shape asymmetry which provides an additional tool to study ultrafast spin dynamics and ratchet-based effects.

DOI: 10.1103/PhysRevB.74.161303 PACS number(s): 78.67.−n, 42.65.Re, 72.15.Lh, 73.23.−b

The spectacular advances in the design and tunability of the time structure, amplitude, phase, and the shape of electromagnetic pulses[1–6] have opened new avenues for their utilization in fundamental and applied research. Inducing and monitoring nonequilibrium states as they build up and decay[7,8] are but one example of recent applications. This progress in laser physics is paralleled with equally impressive development in the fabrication and manipulation of meso- and nanoscale electronic systems in general, and of those with ring-confining geometry in particular.[9–15] Subjecting quantum rings to strongly asymmetric pulses results in the formation of time-dependent charge polarization and charge currents.[16,17] How these nonequilibrium phases collapse, revive, and eventually relax due to coupling to other degrees of freedom has not yet been addressed. We demonstrate that, once the evolution dynamics of the pulse-induced charge polarization is known, a scheme can be developed that allows one to abruptly switch on and off the charge current in the ring, thus enabling a fine tuning of the time structure and the shape of the light-induced current. This is important in so far as the current in the ring is associated with a magnetic field, i.e., controllability of the current allows the generation of short (down to picoseconds) magnetic pulses. The pulse-induced magnetic field can be utilized to study and manipulate locally and in a noninvasive way the picosecond spin dynamics[18] of magnetic samples.[19–22] In addition, we demonstrate how shape asymmetric magnetic pulses can be generated and controlled, revealing thus the potential of our pulses for inducing a ratchet effect without a spatially asymmetric potential.[24] The simplicity of the proposed setup and the local tunability of the magnetic pulse shape and duration make our scheme a valuable addition to currently known accelerator-based methods[19–21] and those based on the generation of currents in two photo switches excited by femtosecond laser pulses.[23]

For inducing nonequilibrium states so-called electromagnetic half-cycle pulses (HCPs)[2–4] are employed. A HCP is a highly asymmetric monocycle pulse whose electric field consists of a strong and short (duration $\tau_d \gtrsim 1$ ps) half cycle followed by a much weaker but longer opposite-polarity half cycle. Collapses and revivals of the HCP-induced nonequilibrium charge polarization, the charge current generation and suppression, and relaxation effects are studied using the density-matrix formalism.[8,25] As we are interested in nondestructive processes, weak HCPs (a few V/cm) are applied. Thus, for low temperatures T, the evolution dynamics is governed by coupling to longitudinal-acoustic (LA) phonons. Electron-electron interaction effects are suppressed by Pauli blocking and energy-conservation restrictions.[26] On the other hand, as we are interested in weak driving fields optical phonons do not influence the evolution dynamics because their energy is well above our highest excited electron energy.

We consider N electrons in an isolated ring with a mean radius r_0, height z_0, and width d $(z_0 \ll d \ll r_0)$ at low T. We specifically address the case where d and z_0 are significantly smaller than the Fermi wavelength of the charge carriers. Hence, only the lowest ground-state radial subbands are populated, a situation that is experimentally feasible for semiconductor-based rings.[30] The single-particle energies associated with the angular motion (characterized by the quantum number m) read $\varepsilon_m = \hbar^2 m^2/(2m^* r_0^2)$, where m^* is the effective mass. The particle angular dynamics is governed by the Hamiltonian $\hat{H}_{\rm tot} = \hat{H}_0^{\rm carr} + \hat{H}_0^{\rm phon} + \hat{H}_{\rm P} + \hat{V}$. Here $\hat{H}_0^{\rm carr} = \Sigma_m \varepsilon_m a_m^\dagger a_m$ is the free-carrier Hamiltonian and $a_m^\dagger$ (a_m) denotes the creation (annihilation) operators. $\hat{H}_0^{\rm phon} = \Sigma_{\vec{q}} \hbar\omega_{\vec{q}} \left(b_{\vec{q}}^\dagger b_{\vec{q}} + \frac{1}{2}\right)$ is the free-phonon Hamiltonian, $\omega_{\vec{q}}$ is the frequency of a phonon with momentum $\vec{q}$, and $b_{\vec{q}}^\dagger$ $(b_{\vec{q}})$ are phonon creation (annihilation) operators. The carrier-phonon coupling is dictated by the Hamiltonian $\hat{H}_P = \Sigma_{\vec{q},m,m'} g_{\vec{q}}^{m'} b_{\vec{q}} a_m^\dagger a_{m-m'} + {\rm H.c.}$, where $g_{\vec{q}}^{m-m'} = g_{\vec{q}}^{\rm bulk} \int d^3r\, \psi_m^*(\vec{r}) e^{i\vec{q}\vec{r}} \psi_{m'}(\vec{r})$ is the electron-phonon coupling constant [25] and $\psi_m(\vec{r})$ are wave functions of the ring carriers in the lowest radial subband. The bulk electron–LA-phonon coupling constant $g_{\vec{q}}^{\rm bulk}$ is determined by $|g_{\vec{q}}^{\rm bulk}|^2 = \hbar |D|^2 q/(2Vc_{\rm LA}\rho_s)$, where D is the deformation constant, $c_{\rm LA}$ is the LA velocity of sound, and ρ_s is the lattice density. The interaction with a time-dependent linearly polarized external electric field $F(t)$ is given by $\hat{V} = -eF(t) r_0 \Sigma_{m,m'} \langle m|\cos\phi|m'\rangle a_m^\dagger a_{m'}$. ϕ identifies the electron angular position with respect to the pulse polarization axis and e is the electron charge.

A key aspect of this work is that the system is excited with a pulse which is very short on the relevant relaxation time scale. Hence, the excitation process can be separated from relaxation and dephasing which occur then in a field-free manner and can be monitored by measuring the emis-

sion spectrum. The excitation dynamics of the system is governed by Heisenberg's equation of motion (EOM) for the density operator $\hat{\rho}_{m,m'}=a_m^\dagger a_{m'}$, i.e., $i\hbar\,\partial_t\hat{\rho}_{m_1,m_2}=[\hat{H}_0^{\rm carr}+\hat{V},\hat{\rho}_{m_1,m_2}]$. In the interaction representation $(\hat{\rho}^{\rm int}_{m_1,m_2}=\hat{\rho}_{m_1,m_2}e^{\frac{i}{\hbar}(\varepsilon_{m_2}-\varepsilon_{m_1})t})$ we find

$$\begin{aligned} i\hbar\,\partial_t\hat{\rho}^{\rm int}_{m_1,m_2}=&-\frac{1}{2}eF(t)r_0\Big(\hat{\rho}^{\rm int}_{m_1,m_2+1}e^{(i/\hbar)(\varepsilon_{m_2}-\varepsilon_{m_2+1})t}\\ &+\hat{\rho}^{\rm int}_{m_1,m_2-1}e^{(i/\hbar)(\varepsilon_{m_2}-\varepsilon_{m_2-1})t}\\ &-\hat{\rho}^{\rm int}_{m_1+1,m_2}e^{(i/\hbar)(\varepsilon_{m_1+1}-\varepsilon_{m_1})t}\\ &-\hat{\rho}^{\rm int}_{m_1-1,m_2}e^{(i/\hbar)(\varepsilon_{m_1-1}-\varepsilon_{m_1})t}\Big). \end{aligned} \tag{1}$$

If the applied pulse duration τ_d is much shorter than $\hbar/(\varepsilon_{m+1}-\varepsilon_m)$, where ε_m is in the vicinity of the Fermi level (E_F) within a range determined by T, then the exponential factors in Eq. (1) hardly vary on the time scale τ_d. For low T this situation is equivalent to $\tau_d\ll\tau_F$ where $\tau_F=2\pi r_0/v_F$ and v_F is the carrier Fermi velocity. This case [called the impulsive approximation (IA)[27,28]] is indeed realizable experimentally: for typical ballistic rings τ_F can be tens of picoseconds, while pulses down to the subpicosecond time scale can be generated with contemporary techniques.[2] Under IA, Eq. (1) reduces in the basis-free form to $i\hbar\,\partial_t\hat{\rho}^{\rm int}=[-eF(t)r_0\cos\phi,\hat{\rho}^{\rm int}]$. If the duration of the negative HCP tail is much longer than τ_F, the action of this tail on the system is averaged to zero. Applying the pulse at $t=0$ we operate again in the Schrödinger picture and derive for the density matrix the relation (for $t>\tau_d$)

$$\rho_{m_1,m_2}=e^{(i/\hbar)(\varepsilon_{m_1}-\varepsilon_{m_2})t}\sum_{mm'}C^*_{m_2,m}C_{m_1,m'}\rho^0_{m',m}, \tag{2}$$

where $\rho^0_{m',m}$ is the density matrix before the application of the pulse. $C_{m_1,m}\equiv\langle m|e^{i\alpha\cos\phi}|m_1\rangle=i^{m_1-m}J_{m_1-m}(\alpha)$, $J_l(x)$ are Bessel functions, and $\alpha=r_0p/\hbar$, where $p=-e\int_0^{\tau_d}F(t)dt$ is the momentum transferred to the charge carriers. If for $t<0$ the system is in an equilibrium state then the initial density matrix $\rho^0_{m',m}=f^0_m(\eta,T)\delta_{m',m}$, where $f^0_m(\eta,T)$ is the Fermi-Dirac distribution function (η and T denote the chemical potential and the temperature, respectively).[31] For our isolated rings the chemical potential at a given temperature is uniquely determined by the number of particles in the ring N. The pulse electric field is chosen as $F(t)=F_0(t/\tau_0)[\exp(-t^2/2\tau_0^2)-(1/b^2)\exp(-t/b\tau_0)]$. The parameters F_0, τ_0, and b determine, respectively, the amplitude, the duration, and the asymmetry of the pulse. The duration τ_d of the positive half cycle is determined by $\tau_d=\tau_0(1+\sqrt{1+2b^2\ln b^2})/b$. For $b=8$ the pulse has basically the experimentally observed shape and ratio of 13:1 between the maximum field values of the positive and negative polarity parts.[2] The peak field strength is $F_p\approx0.593F_0$. When rings are irradiated with these pulses, a charge polarization builds up that is characterized by the dipole moment $\vec{\mu}(t)=\mathrm{Tr}[e\vec{r}\hat{\rho}(t)]$. The components of the dipole moment along and perpendicular to the pulse polarization are $\mu_\parallel(t)=er_0\Sigma_m\mathrm{Re}[\rho_{m+1,m}]$ and $\mu_\perp(t)=er_0\Sigma_m\mathrm{Im}[\rho_{m+1,m}]$, respectively. A detailed comparison between the dynamics of the dipole moment calculated using the IA and the exact numerical solution for different τ_d but fixed α endorsed our expectation that the IA is well justified if τ_d is smaller than a quarter period of the dipole moment oscillations (a period of oscillation is determined by the energy difference between levels near E_F) and the HCP tail duration is longer than a quarter period of oscillations. Thanks to the IA a single parameter, the kick strength α, is sufficient for characterizing the coupling of the HCP to the electronic system.

The non-equilibrium dynamics of the induced dipole moment is inferred from the EOM for ρ_{m_1,m_2} (including scattering from phonons), i.e.,[25]

$$\begin{aligned} i\hbar\,\partial_t\rho_{m_1,m_2}=&(\varepsilon_{m_2}-\varepsilon_{m_1})\rho_{m_1,m_2}+\sum_{m_3\vec{q}}[g_{\vec{q}}^{m_2-m_3}s_{\vec{q}}^{m_1,m_3}\\ &+(g_{\vec{q}}^{m_3-m_2})^*(s_{\vec{q}}^{m_3,m_1})^*-g_{\vec{q}}^{m_3-m_1}s_{\vec{q}}^{m_3,m_2}\\ &-(g_{\vec{q}}^{m_1-m_3})^*(s_{\vec{q}}^{m_2,m_3})^*]. \end{aligned}$$

Using the Markov approximation and neglecting polaron corrections the phonon-assisted density matrices $s_{\vec{q}}^{m_1,m_2}\equiv\langle b_qa^\dagger_{m_1}a_{m_2}\rangle-\langle b_q\rangle\langle a^\dagger_{m_1}a_{m_2}\rangle$ in absence of an external mechanical action read[25]

$$\begin{aligned} s_{\vec{q}}^{m_1,m_2}=&-i\pi\delta(\varepsilon_{m_2}-\varepsilon_{m_1}+\hbar\,\omega_{\vec{q}})\sum_{m_3,m_4}(g_{\vec{q}}^{m_4-m_3})^*\\ &\times[(n_{\vec{q}}+1)\rho_{m_1,m_4}\bar{\rho}_{m_3,m_2}-n_{\vec{q}}\rho_{m_3,m_2}\bar{\rho}_{m_1,m_4}], \end{aligned}$$

where $\bar{\rho}_{m,m'}\equiv\delta_{m,m'}-\rho_{m,m'}$. For $\alpha<1$, i.e., for weak excitations, we write $\rho_{m_1,m_2}\approx f^0_{m_1}\delta_{m_1,m_2}+\tilde{\rho}_{m_1,m_2}$. Assuming thermal equilibrium for phonons [i.e., $n_{\vec{q}}\equiv n^0(q)$, where $n^0(q)$ is the Bose-Einstein distribution function], performing the sums over $\vec{q}$, and assuming the Debye model for the LA-phonon spectrum, we arrive at the equation for our numerical calculations of the relaxation dynamics:

$$\begin{aligned} \partial_t\tilde{\rho}_{m_1,m_2}=&\left[\frac{i}{\hbar}(\varepsilon_{m_1}-\varepsilon_{m_2})-\sum_m\frac{R^m_{m_1}+R^m_{m_2}}{\tau_{\rm LA}}\right]\tilde{\rho}_{m_1,m_2}\\ &+\sum_m\frac{\tilde{\rho}_{m_1+m,m_2+m}}{\tau_{\rm LA}}\left(R^{m_1}_{m_2+m}+R^{m_2}_{m_1+m}\right), \end{aligned} \tag{3}$$

where $\tau_{\rm LA}=\hbar c^2_{\rm LA}\rho_sd^2r_0/|D|^2$,

$$R^m_{m'}=\begin{cases}\mathcal{F}^{m'}_m(q^m_{m'},d)[n^0(q^m_{m'})+f^0_m], & q^m_{m'}\in\left(0,\dfrac{\omega_{\rm D}}{c_{\rm LA}}\right),\\ \mathcal{F}^{m'}_m(q^m_{m'},d)[n^0(q^m_{m'})+1-f^0_m], & q^m_{m'}\in\left(-\dfrac{\omega_{\rm D}}{c_{\rm LA}},0\right),\\ 0 & \text{otherwise;}\end{cases} \tag{4}$$

$q^m_{m'}=(\varepsilon_m-\varepsilon_{m'})/(\hbar c_{\rm LA})$ and $\omega_{\rm D}$ is the Debye frequency; $\mathcal{F}^{m'}_m(y)=8\pi^2y\int_0^y dx(1/\sqrt{1-x^2/y^2})\sin^2(x/2)/(x^2[x^2-(2\pi)^2]^2)$ if $\mathrm{sgn}(m)=\mathrm{sgn}(m')$ and $\mathcal{F}^{m'}_m(y)=0$ otherwise.

The short-pulse-induced dynamics occurs within the fol-

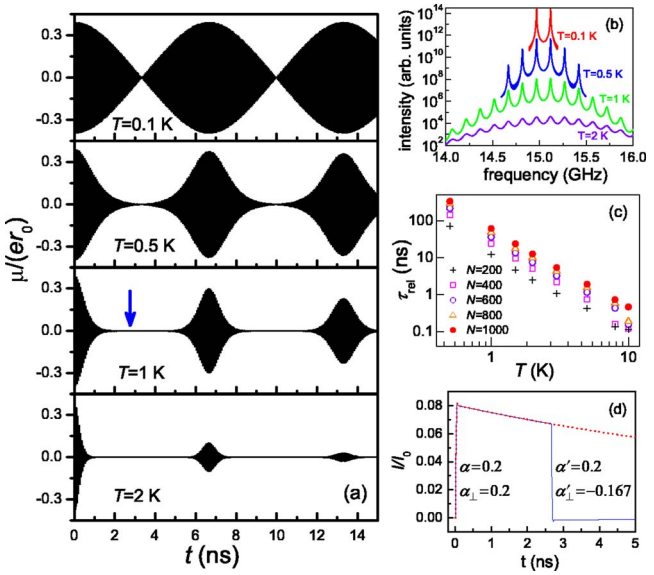

FIG. 1. (Color online) (a) Dynamics of the dipole moment μ for different temperatures. Kick strength $\alpha=0.2$. (b) Emission spectra. The curves are offset vertically for clarity. (c) Dependence of the relaxation time of the dipole moment on temperature T and the number N of electrons. (d) Numerically calculated current decay (dotted line) after excitation by the $T_{\mathrm{cl}}/4$-delayed sequence of two mutually perpendicular HCPs and current suppression (full line) by application of the second $T_{\mathrm{cl}}/4$-delayed sequence. Duration of each HCP is $\tau_d=3$ ps; $T=1$ K. The arrow in (a) marks the time moment when the stopping sequence of HCPs is applied. Parameters of the ring: $r_0=1.35$ μm, $d=50$ nm, and $N=400$.

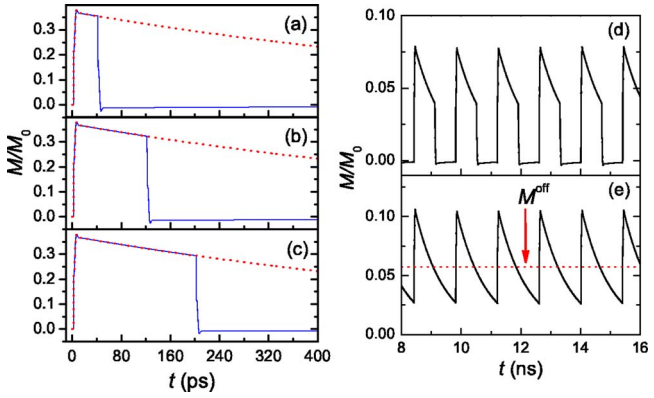

FIG. 2. (Color online) (a) Magnetization pulses generated in the ring by application of two HCP pairs delayed by $\tau_{p-p}=40$, (b) 120, (c) 200 ps. Kick strengths are $\alpha_{\parallel}=\alpha_{\perp}=\alpha'_{\parallel}=0.4$, $\alpha'_{\perp}=-0.39$ in (a), −0.35 in (b), and −0.32 in (c). Magnetization M is normalized to $M_0=\pi r_0^2 I_0$. Dotted lines show the result without applying the second HCP pair. Parameters of the calculation: $r_0=0.3$ μm, $d=20$ nm, $N=160$, $T=20$ K, $\tau_d=0.5$ ps. (d) and (e) show periodically alternating time-asymmetric magnetization generated in the ring by application of series of sequences of HCPs with a time delay between sequences of 1.4 ns. In (d) each sequence contains four HCPs having kick strengths $\alpha_{\parallel}=0.2, \alpha_{\perp}=0.2, \alpha'_{\parallel}=0.2$, and $\alpha'_{\perp}=-0.1$, respectively. In (e) each sequence contains two HCPs having kick strengths $\alpha_{\parallel}=0.2$ and $\alpha_{\perp}=0.2$, respectively. M^{off} is the offset magnetization associated with an external magnetic field [24]. Parameters of the ring and duration of HCPs as in Fig. 1, $T=4$ K.

lowing scenario. Starting from the ground state a short pulse drives the system to the excited state determined by Eq. (2). This nonequilibrium state serves as the initial condition for the numerical propagation of Eq. (3), which in turn governs the postpulse charge dynamics.

For the calculations the following ring material parameters (corresponding to n-GaAs) are employed: $c_{\mathrm{LA}}=4.79\times10^5$ cm/s, $\rho_s=5.32$ g/cm^{-3}, $|D|=8.6$ eV, $\hbar\omega_{\mathrm{D}}=30$ meV, $m^*=0.067m_0$ (m_0 is the free-electron mass). Figure 1(a) shows the nanosecond dynamics of the dipole moment μ for $N=400$ and different T (the oscillatory behavior on the much shorter time scale τ_F is not resolved[16]). For low T (=0.1 K) only states with two possible energy values near the E_F are populated. The long-time behavior thus exhibits beatings, and hence two peaks in the emission spectrum [Fig. 1(b)] are observable. With increasing T more levels near E_F are populated and the dynamics of the dipole moment shows alternating collapsed states and quantum revivals. The revival time is given by $T_{\mathrm{rev}}=4\pi\hbar/|\partial^2\varepsilon_m/\partial m^2|$ with ε_m in the proximity of E_F. The fast (classical) oscillations have a period $T_{\mathrm{cl}}=2\pi\hbar/|\partial\varepsilon_m/\partial m|\approx\tau_F$.[29] The decay of the revival peak values is due to the relaxation. For an estimate of the dipole-moment relaxation time, τ_{rel}, we utilize the decay dynamics and use the two first consecutive envelope maxima to determine τ_{rel} from a fit by $A\exp(-t/\tau_{\mathrm{rel}})$. Figure 1(c) displays the dependence of τ_{rel} on T and on the number of electrons N in the ring. τ_{rel} increases rapidly with decreasing T and, as expected, τ_{rel} tends to infinity for $T\to0$. Figure 1(b) evidences that by measuring the emission spectrum the temperature-dependent decay dynamics can be traced. The different decay dynamics of the dipole moment and of the current (which can be monitored separately) allows insights into different parts of the density matrix. The dipole moment (current) is determined namely by the diagonal (near-diagonal) elements of the density matrix.

Applying two time-delayed mutually perpendicular HCPs generates charge current I and an associated magnetization M in the ring.[17] The utilization of the pulse-induced magnetic field to monitor locally, in a pump-probe manner, the ultrafast spin dynamics in nanostructures or to induce a fast ratchet effect requires a fine control of the fast switching behavior of the pulse-triggered magnetic field, a task that is tackled here by utilizing the collapsed states of the dipole moments. Two weak perpendicular pulses with strengths $\alpha_{\parallel}$ and $\alpha_{\perp}$ and delay time τ (chosen as $\tau=T_{\mathrm{cl}}/4$) initiate along the respective field axis two independent polarization dynamics $\mu_{\parallel}(t)$ and $\mu_{\perp}(t)$. Using Eq. (2) we derive that the charge current change ΔI by application of the second HCP with kick strength $\alpha_{\perp}$ at $t=t_{\mathrm{sw}}$ is given by

$$\Delta I=-\alpha_{\perp}\frac{\mu_{\parallel}(t=t_{\mathrm{sw}}^-)}{er_0}I_0,\quad I_0=e\hbar/(m^*r_0^2). \tag{5}$$

Correspondingly, the ring magnetization is shifted by $\Delta M=\pi r_0^2\Delta I$, and the current-generated magnetic flux by $\Delta\Phi=(\pi/2)\mu_0 r_0\Delta I$ (μ_0 is the magnetic permeability of surrounding material). Equation (5) can be exploited to turn the current on and off, thus producing short magnetic pulses, as

follows. Having produced a current with a HCPs pair we subject (after the time $\tau_{p\text{-}p}$) the collapsed state to a second sequence of two pulses. The first pulse of the second sequence has the strength $\alpha' = \alpha_{\|}$ and triggers the same dynamics of the dipole moment as does the first HCP of the first HCPs pair because the collapsed state is unpolarized. The second pulse of the second sequence has strength $\alpha'_{\perp}$ and is applied with polarity opposite to the second HCP of the first pair. $|\alpha'_{\perp}|$ is chosen smaller than $\alpha_{\perp}$ by a factor determined by the current decay during $\tau_{p\text{-}p}$ and in such a way that the currents triggered by the two HCP pairs cancel each other. Figure 1(c) demonstrates numerically the accuracy of this scheme of current switching. The abrupt current switching opens the way for the tunability of the time structure of the magnetic pulses. The magnetic pulses duration is stretchable depending on $\tau_{p\text{-}p}$ [cf. Figs. 2(a)–2(c)]: As inferred from Figs. 1(d) and 2(a)–2(c), if $\tau_{p\text{-}p} \ll \tau_{\mathrm{rel}}^{\mathrm{cur}}$, where $\tau_{\mathrm{rel}}^{\mathrm{cur}}$ is the time constant for the current initial decay dynamics, almost rectangular ps magnetic pulses are produced. For $\tau_{p\text{-}p} \gtrsim \tau_{\mathrm{rel}}^{\mathrm{cur}}$ asymmetric pulses are triggered, which is of importance when studying ratchet effects.[24] Figure 2 demonstrates the level of tunability of the pulse shape and duration by varying experimentally accessible parameters. The magnitude of the triggered pulses is enlarged for smaller rings and/or stronger kicks. Also an appropriate arrangement of a collection of rings allows additional tuning of the magnetic pulses.

In summary, we demonstrated how relaxation, collapses, and revivals in quantum rings can be studied by means of electromagnetic pulses and how these phenomena can be exploited to generate with current technology magnetic pulses with tunable time and shape structure. Numerical calculations with realistic pulse and material parameters are performed, endorsing the feasibility of the predicted effects with current technology.

*Also at A. F. Ioffe Physico-Technical Institute, 194021 St. Petersburg, Russia. Electronic address: moskalen@mpi-halle.de

[1] A. M. Weiner, D. E. Laird, J. S. Patel, and J. R. Wullert, Opt. Lett. **15**, 326 (1990); M. M. Wefers and K. A. Nelson, *ibid.* **18**, 2032 (1993).

[2] D. You, R. R. Jones, P. H. Bucksbaum, and D. R. Dykaar, Opt. Lett. **18**, 290 (1993); N. E. Tielking, T. J. Bensky, and R. R. Jones, Phys. Rev. A **51**, 3370 (1995).

[3] T. J. Bensky, G. Haeffler, and R. R. Jones, Phys. Rev. Lett. **79**, 2018 (1997).

[4] G. L. Carr, M. C. Martin, W. R. McKinney, K. Jordan, G. R. Neil, and G. P. Williams, Nature (London) **420**, 153 (2002); M. Sherwin, *ibid.* **420**, 131 (2002).

[5] T. Brabec and F. Krausz, Rev. Mod. Phys. **72**, 545 (2000); R. E. Slusher, *ibid.* **71**, S471 (1999).

[6] T. Brixner, G. Krampert, T. Pfeifer, R. Selle, G. Gerber, M. Wollenhaupt, O. Graefe, C. Hom, D. Liese, and T. Baumert, Phys. Rev. Lett. **92**, 208301 (2004).

[7] R. Huber, F. Tauser, A. Brodschelm, M. Bichler, G. Abstreiter, and A. Leitenstorfer, Nature (London) **414**, 286 (2001).

[8] H. Haug and S. W. Koch, *Quantum Theory of the Optical and Electronic Properties of Semiconductors* (World Scientific Publishing, London, 2004).

[9] D. Mailly, C. Chapelier, and A. Benoit, Phys. Rev. Lett. **70**, 2020 (1993).

[10] A. Fuhrer, S. Lüscher, T. Ihn, T. Heinzel, K. Ensslin, W. Wegscheider, and M. Bichler, Nature (London) **413**, 822 (2001).

[11] A. Lorke, R. J. Luyken, A. O. Govorov, J. P. Kotthaus, J. M. Garcia, and P. M. Petroff, Phys. Rev. Lett. **84**, 2223 (2000).

[12] W. Rabaud, L. Saminadayar, D. Mailly, K. Hasselbach, A. Benoît, and B. Etienne, Phys. Rev. Lett. **86**, 3124 (2001).

[13] P. Mohanty, Ann. Phys. (N.Y.) **8**, 549 (1999).

[14] E. M. Q. Jariwala, P. Mohanty, M. B. Ketchen, and R. A. Webb, Phys. Rev. Lett. **86**, 1594 (2001).

[15] M. Kläui, C. A. F. Vaz, J. A. C. Bland, L. J. Heyderman, F. Nolting, A. Pavlovska, E. Bauer, S. Cherifi, S. Heun, and A. Locatelli, Appl. Phys. Lett. **85**, 5637 (2004); M. Kläui, C. A. F. Vaz, J. A. C. Bland, W. Wernsdorfer, G. Faini, E. Cambril, L. J. Heyderman, F. Nolting, and U. Rüdiger, Phys. Rev. Lett. **94**, 106601 (2005).

[16] A. Matos-Abiague and J. Berakdar, Phys. Rev. B **70**, 195338 (2004).

[17] A. Matos-Abiague and J. Berakdar, Phys. Rev. Lett. **94**, 166801 (2005).

[18] B. Hillebrands and K. Ounadjela, *Spin Dynamics in Confined Magnetic Structures* (Springer, Berlin, 2003).

[19] C. H. Back, R. Allenspach, W. Weber, S. S. P. Parkin, D. Weller, E. L. Garwin, and H. C. Siegmann, Science **285**, 864 (1999).

[20] Y. Acremann, C. H. Back, M. Buess, O. Portmann, A. Vaterlaus, D. Pescia, and H. Melchior, Science **290**, 492 (2000).

[21] I. Tudosa, C. Stamm, A. B. Kashuba, F. King, H. C. Siegmann, J. Stohr, G. Ju, B. Lu, and D. Weller, Nature (London) **428**, 831 (2004).

[22] D. Atkinson, D. A. Allwood, G. Xiong, M. D. Cooke, C. C. Faulkner, and R. P. Cowburn, Nat. Mater. **2**, 85 (2003).

[23] Th. Gerrits, H. A. M. van der Berg, J. Hohlfeld, L. Bar, and T. Rasing, Nature (London) **418**, 509 (2002).

[24] D. Cole, S. Bending, S. Savel'ev, A. Grigorenko, T. Tameqai, and F. Nori, Nat. Mater. **5**, 305 (2006).

[25] F. Rossi and T. Kuhn, Rev. Mod. Phys. **74**, 895 (2002).

[26] T. Chakraborty and P. Pietiläinen, Phys. Rev. B **50**, 8460 (1994).

[27] N. E. Henriksen, Chem. Phys. Lett. **312**, 196 (1999).

[28] D. Daems, S. Guerin, H. R. Jauslin, A. Keller, and O. Atabek, Phys. Rev. A **69**, 033411 (2004).

[29] R. W. Robinett, Phys. Rep. **392**, 1 (2004).

[30] Generalization to multiple radial channels can be handled in a similar way; A. Matos-Abiague and J. Berakdar, Europhys. Lett. **69**, 277 (2005).

[31] Many-body effects on the ground-state distribution function are suppressed due to Pauli's principle.